

Environmentally Friendly Synthesis, Antibacterial Activity, and Photocatalytic Performance of Ag Nanoparticles Made from *Leucaena Leucocephala* Leaves Extract

KARRAR HAZIM¹, GHUSOON FAIDHI HAMEED², LIDIA MOHAMED³, FARIS J. ALYASIRI⁴

¹Pharmacy Department, Al-Mustaqbal University College, 51001 Hillah, Babil, Iraq

²Department of Chemistry, Faculty of Education, Al-Qadisiyah University, Al-Qadisiyah, Iraq

³Al-Zahrawi University College/ Department of Medical lab-technology

⁴Islamic Azad university science and research branch

Corresponding author, Karrar Hazim, Email: karrar.hazim@mustaqbal-college.edu.iq

ABSTRACT

The leaf extract of the plant *Leucaena leucocephala* was used in this research to synthesize environmentally-friendly nanotechnologies. This environmentally friendly procedure is completely safe and non-toxic. The approach is cost-effective, simple to use, and effective, and the attributes of the resultant compounds can be regulated. For example, the Ag compound can be controlled using the same plant extract and reaction. The findings and properties of these nanoparticles were investigated using a variety of techniques, including field emission-scanning electron microscopy (FE-SEM), X-ray diffraction (XRD), and atomic force microscopy (AFM). EDX-mapping was also used to explore the analysis of Ag NPs. Electron microscopy investigations with transmission electron microscopes (TEM). which indicated the presence of Ag in the compound and their effective degradation. The produced chemical was tested for effectiveness using bacteria. The antibacterial activity of Ag NPs was investigated utilizing two different species of bacteria, Gram-negative *E. Coli* and Gram-positive *S.aureus* e.In addition, the photocatalytic capacity of Ag NPs was discovered through the photodegradation of dyes, as the rhodamine B dye was decomposed at a 78% percent rate. The effect of the catalyst amount and amounts (0.2,0.4,0.6,0.8,1, 1.2,1.4,1.6g/L) were investigated, with the best weight being 1gm and the dye concentration being 10ppm. Water and oxygen are converted to OH radical with very powerful oxidation by receivers for electrons as well as those electrons and free holes.

Keywords: Ag NPs; photocatalytic degradation; anti-bacterial activity; *Leucaena leucocephala*;

INTRODUCTION

Environmental pollution is one of the main problems of the world, which includes soil pollution, air, and water. This problem has increased in recent years due to increased population density, and many factories, so the development of this problem is to be prevented by quality control Environmental monitoring, one of the most important methods of monitoring, biological method, which includes monitoring many plants, trees, fish as well as bacteria and viruses as indicators in environmental quality control[2 ,1] . the waste is one of the most important pollutants that affect the environment that leads to changes in environmental quality, soil, and air that affect Plant, animal life and microorganisms [3] . pollution is heavy metal elements of the most affected species such as chromium and arsenic ions, carcinogens and absorbs by the digestive system of man through the skin when touching them[4]. The problem of water pollution is one of the main problems due to increased organic chemical pollutants and membership used in industrial activities, including toxic minerals organic pollutants, waste sites, and more dangerous mining operations on sewage pollution. where these pollutants are changing the physical characteristics and increase the amount of impurities in the water [5]. biological methods are one of the most important techniques that have proved to remove pollutants from contaminated water because of good performance and low cost. Industrial waste in water reduces the reimbursement of chemicals that cause a significant danger to the environment because of their nodule, instability, and lack of validity, so researchers have resorted to the use of environmentally friendly biological roads, which provide a large amount of production, as well as non-toxic and low cost[6, 7]. Photocatalysis is one of the most effective wastewater treatment procedures due to its benefits over other approaches, such as fast and practically full destruction of wastewater contaminants and no creation of toxic intermediates and by-products [8]. the synthesis in environmentally friendly nanotechnologies using the leaf extract of the plant *Leucaena leucocephala*. This eco-friendly method is safe and non-toxic or harmful to the environment one of the most important techniques used to address water pollution of homogeneous and non-homogeneous immunity stimulus in the effect of the sunlight[9]. Polluted and then get rid of dyes, these oxidations are used to remove vehicle pollutants, through analyzing and smashing

formalized and phenolic pollutants from contaminated water, and there is another way to get rid of organic pollutants such as nanoscale method[10]. Silver is one of the transition metals, and it is a metal with a color between white and gray, and it is one of the nanoparticles that are of great importance because of its properties, including thermal conductivity and electrical conductivity [11]. in addition to the shape and size and it is prepared in an environmentally friendly way to overcome obstacles and the disadvantages of preparing it by chemical methods and the environmentally friendly method provides ease of preparation and low cost and dependence on materials that do not pollute the environment and this method is important in preparing nano-silver and this method provides more ability to control the size and shape through pH, temperature and reducing agents[12, 13]. Either inorganic materials anti-bacteria are characterized by high stability and unique size in which large surface space is no surface area to size and this increasing surface of the nanoparticles enhances the interaction with the surrounding molecules as well as stimulate the death of genuine cells as well as the growth in cells The primitive kernel is torn by bacteria and fungal grease layers[14, 15]. which leads to the discharge of the contents of cytoplasm because of the poisonous behavior of nanotechnology, Among metallic NPs, Ag NPs are one of the most biotic and intriguing nanomaterials[16]. Ag NPs are used in a variety of medicinal and therapeutic procedures. Ag NPs have proved incredibly beneficial in a variety of sectors of study, including biology, biomedicine, chemical engineering, the environment, and many others, due to their unique features [17]. It's also important in nanotechnology and nanoscience, particularly in nanomedicine. Antimicrobial, anticancer, antioxidant, and anti-inflammatory characteristics of silver nanoparticles have opened up a wide range of applications for these nanoparticles in biomedicine. Many common synthetic approaches for manufacturing Ag NPs[18]. Chemical preparation methods, on the other hand, have several disadvantages, including high energy consumption, high expense, and the potential for harmful substances or dangerous physical therapies. In recent years, there has been a worldwide movement toward more environmentally friendly nano catalyst manufacturing procedure. Plant extracts, bacteria, fungi, and algae have all been employed in various ways to biosynthesize Ag NPs. Ag NPs have been reported to be made from a variety of plant extracts, including roots, flowers, leaves,

stems, seeds, and fruits. To evaluate the material, researchers employed X-ray diffraction (XRD), scanning electron microscopy (FE-SEM), energy-dispersive X-ray spectroscopy (EDX), transmission electron microscopy (TEM), and atomic force microscopy (AFM).

Experimental details

MATERIAL AND MATERIALS

Silver nitrate (AgNO_3 , 99 percent) and Rhodamine B (empirical formula: $\text{C}_{28}\text{H}_{31}\text{ClN}_2\text{O}_3$; dye content 97 percent; max = 553 nm) were acquired from Sigma-Aldrich and utilized without additional purification. Ethanol ($\text{C}_2\text{H}_5\text{OH}$, 99.5%) is a kind of alcohol. All of the solutions were made with deionized water (DI).

Characterization of Ag NPs: The crystal phase of nanomaterial was tested via was determined using a Shimadzu XRD 6000 diffractometer and Ni-filtered Cu K irradiation ($\lambda = 1.54056$) in the 10° – 80° range. Transmission electron microscopy (TEM, Hitachi H-9500) and field emission-scanning electron microscopy were used to examine the morphology and size of as-prepared nanomaterials (FE-SEM, MIRA3 TESCAN, Czech). The elemental composition of surfaces of as produced nanomaterials was determined using an energy dispersive X-ray diffraction spectroscopy (EDX) linked to a FE-SEM. To identify functional groups and characterize the molecular structures of as produced nanomaterials, researchers employed an FTIR Shimadzu 8400s spectrophotometer (Japan) with KBr-pressed disks and a spectrum range of 4000 – 500 cm^{-1} . The roughness of the surface was measured using an Angstrom AFM (SPM-AA3000, USA)

Preparing the plant extract: A 10 g of fresh leaves of *Leucaena leucocephala* are rinsed with deionized water (DIW) to eliminate dust and then processed to a very fine powder using an electric grinder under normal conditions. and submerged in 100 mL of water (DIW). To obtain the plant extract, the solution was boiled for 30 minutes at 80°C , then filtered to eliminate fine suspended particles. The clear extract was then kept at 4°C until it could be employed in the biosynthesis of Ag NPs.

Biosynthesis Silver nanoparticles: Ag nanoparticles were synthesized 0.5 g of AgNO_3 was typically dissolved in 50 mL of aqueous *Leucaena leucocephala* extract, then reduced into AgNO_3 by continuous magnetic stirring at 80°C for about 4 hours. To avoid photoreactions, the solution was then covered with a dense aluminum foil and kept at room temperature for 24 hours. For 20 minutes, the reaction mixture was centrifuged at 6000 rpm. To eliminate any adsorptive impurities, the brown-colored precipitate was repeatedly washed with DI and ethanol DIW, then dried at 80°C for 4 hours to get a pale white solid. The color change from yellow to white confirmed the reduction of silver nitrate to silver ions. The solid was resulting.

Degradation of the RhB dye by photocatalysis: To obtain the adsorption-desorption equilibrium of dye molecules on the Ag surface, a solution containing Ag NPs and dye was magnetically agitated for 180 minutes in darkness. A visible light source of a 200 W Xenon lamp and a temperature controller were included in the photoreactor. The bulb was placed about 10 cm above the reaction mixture in the middle of the reactor. To achieve the adsorption/absorption equilibrium of dye molecules on the surface of the photocatalyst, 50 mL of 10 ppm Rh. B was placed in a beaker, and a defined amount of photocatalyst was suspended into the dye solution and ultrasonically treated for 15 minutes, then subjected to continuous stirring for 180 minutes in the dark.

$$\text{PDE}\% = \frac{A_0 - A}{A} \times 100\% \quad (1)$$

The absorbance of RhB at zero and at the time (t) are represented by A_0 and A, respectively. Various operating parameters, such as catalyst dosage (0.2–1.8 g/L) and beginning dye concentration, influence degradation efficiency (10 ppm).

DISCUSSION OF THE FINDINGS

Diffraction of X-rays (XRD): The crystalline characteristics of Ag nanoparticles are shown in Figure 1. X-ray diffraction in the 20 – 80° range was used to identify silver nanoparticles. The measurements reveal that the silver is in a crystalline phase, with more intense peaks at 38.0438° , 46.4031° , 64.3769° , and 78.3003° , respectively, corresponding to the lattice (hkl) planes (111), (200), (220), and (311) crystal of face-centered cubic structure of Ag crystalline (JCPDS profile 004-0723). (X-Ray Diffraction) The crystal form is determined using XRD technology [19]. Table 1 shows the results of utilizing the Debye-Scherrer equation to calculate crystalline size

$$D = \frac{K\lambda}{\beta \cos\theta} \quad (2)$$

Where D is crystallite size, K is a constant of 0.9, X-ray radiation wavelength ($\lambda = 1.54$), full width at half maximum (FWHM of XRD peaks), and diffraction angle are all constants.

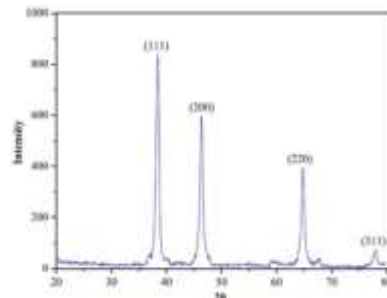


Figure 1: XRD diffraction patterns of Ag

Table 1: Data of XRD pattern for the synthesized Ag NPs

No.	Pos. [2θ]	FW HM	d-spacing [Å]	Rel. Int. [%]	Lattice Strain	Average Size (nm)
1	38.0438	0.2917	2.48779	12.42	0.0062	
2	46.4031	0.3019	2.75085	15.64	0.0040	35
3	64.3769	0.2163	2.49196	31.82	0.0029	
4	78.3003	0.1528	2.73731	11.05	0.0034	

Fourier transform infrared spectroscopy (FT IR): The FT-IR measurements had been investigated in the range 400 – 4000 cm^{-1} to approve and identify the formation of Ag as shown in Figure (2). In FTIR of pure Ag nanoparticles, the absorption bands of metal usually appear in the fingerprint region below 1000 cm^{-1} arising from inter-atomic vibrations. The peak at 663.03 cm^{-1} is corresponding to (Ag) stretching and distortion vibration, respectively. The absorption stretch band present at 3342 and 3354 cm^{-1} correspond to the surface-adsorbed hydroxyl groups (O–H) and water. The absorption band presented at 511 , 523 , and 533 cm^{-1} (Ag), where it is noted that it is lower than the values of absorption of pure Ag[20].

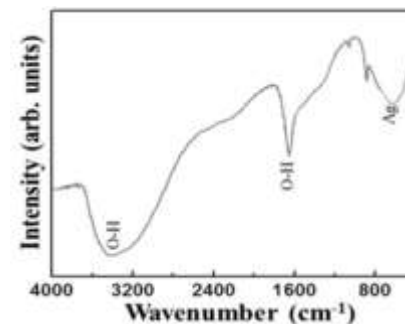


Figure 2: FTIR spectra of Ag

(AFM) Atomic Force Microscopy :The AFM, roughness average, surface skewness, surface kurtosis, and average diameter were used to investigate the surface attributes of Ag nanoparticles. The shapes of Ag nanoparticles were almost homogenous distribution and a small aggregation, as illustrated in Figure (3), and the surface had valleys rather than peaks and barbed character. A range's average diameter is (20-85) nm. Because the Rku is less than 3, the surface shape is flat. Because the Rsk is negative, the surface is flat. and the average beacons (Ra) is 6.18 and the root of the average Rq squared Rq is 7.23, which indicates that the declines are greater than altitudes. The class has a thickness of 27.00 millimeters. The forms of the two- and three-dimensional images, as well as the grain distribution rate, silver, were examined using atomic force microscopy AFM. The AFM image revealed that the shapes of the silver particles are nearly uniform, with deep gaps in the surface[21].

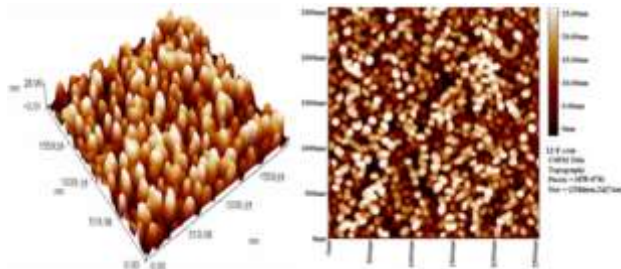


Figure 3: 3D and 2D image of AFM for AgNPs

Field-Emission Scanning Electron Microscopy (FE-SEM): The surface morphology of Ag nanoparticles was studied using the FE SEM. Ag nanoparticles can be observed as cubic or spherical with uniform distribution in the FE-SEM image displayed in Figure 3, and agglomeration can also be seen as randomly dispersed FE-SEM images highlight the creation of nanostructures with porous surfaces. The shape of the biosynthesized AgNPs was visible in FE-SEM images. The average diameter is (20-85) nm, which matches the XRD result well[22].

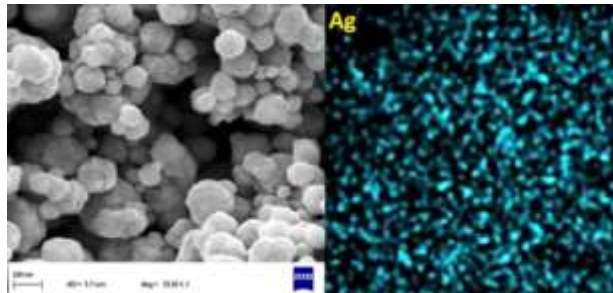


Figure 4: FE-SEM Images of the Ag and Images representing the elements silver

Transmission Electron Microscopy (TEM): The size of the particles, their development pattern, and the distribution of the crystallite were all confirmed using transmission electron microscopy. Figure(6) shows a TEM picture of Ag nanoparticles. These nanoparticles have virtually cubic-like geometries with well-defined borders, as shown in the TEM image. The average size of the nanoparticles as determined directly from the image is 30 nm, as shown in the micrographs[23].

Elemental analysis (EDX) :The presence of the green-made silver element was proven by EDX analysis, and the EDX results confirmed the presence of very pure Ag NPS. Figure (7) of the EDX analyses that were used to determine the proportion of elements in the width of the Ag sample and the presence of the green-made silver element was proven by EDX analysis. One of the markers that Ag NPs are formed is the atomic ratio 100% and

the weight ratio of 100% of silver. This verifies that Ag NPs are formed. Previous research has shown that the synthetic compound is an extremely pure nanocomposite with no impurities[24].

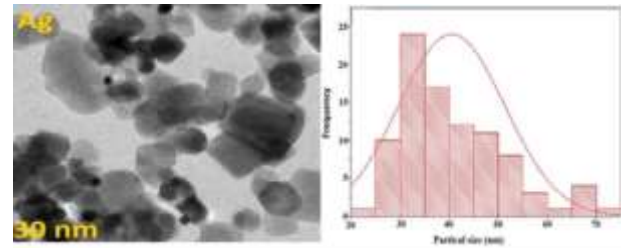


Figure 5: TEM analysis and Histogram of TEM analysis

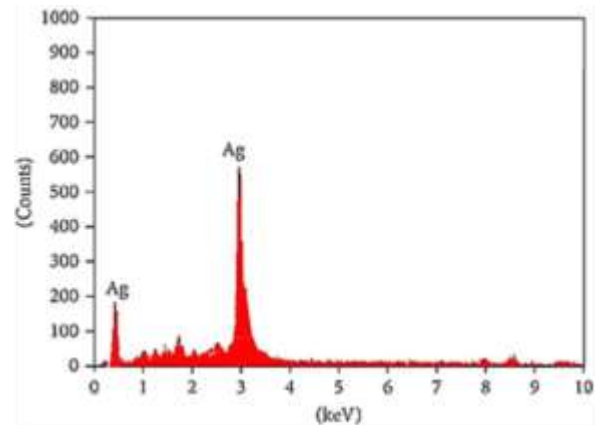


Figure 6: represents EDX for the Ag

Antibacterial Assay :Two varieties of bacteria were utilized to evaluate the biological activity of the produced compounds: one is (*Escherichia coli*), which is negative for the chromium dye, and the other is (*Staphylococcus aureus*), which is positive for the chromium dye. The results revealed that silver had antibacterial action against *E. coli* and *S. aureus* at two distinct doses (0.001, 0.0005 g/mL) and that the results were varied, with silver showing good resistance against both bacteria by disrupting and tearing bacterial membranes. These actions are dependent on the type of nanomaterials and bacteria used. Furthermore, various factors, such as oxidative stress, genomic and plasmid DNA factors, and degradation factors, can harm or kill bacteria, and it was reported that [25, 26].

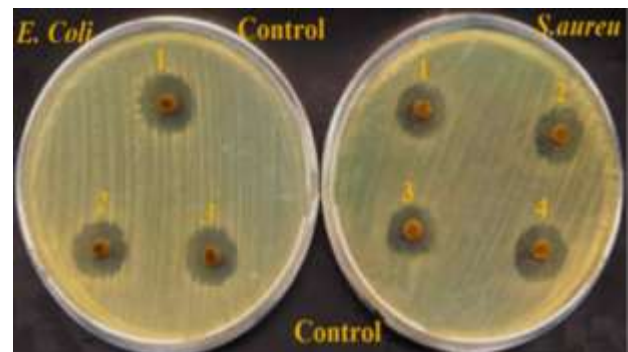


Fig 7: represents the effect of Ag NPs on *E. Coli* bacteria and bacteria *S. aureus*

Effect of photocatalyst dose: A series of experiments to determine the best amount of the catalyst revealed that the amount in which the catalyst performed best was 1g/L, where the quantities tested were 0.2g, 0.4g, 0.6g, 0.8g, 1g, 1.2g, 1.4, 1.8 g).

It was discovered that the catalyst's efficiency increases with the increase in the amount of the catalyst until a specific amount is reached, after which the catalyst's efficiency begins to decrease with the increase in the amount of the catalyst[27].

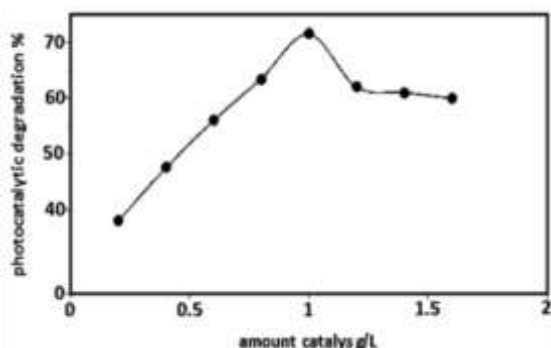


Fig 8: Effect of the amount of photocatalyst on the photodegradation efficiency process (dye concentration 10ppm, temperature 30°C, irradiation time 180minutes).

Mechanism of Ag NPs Action: Silver nanoparticles' specific mechanism of action on cells is uncertain. However, a substantial amount of evidence has accumulated in this area, particularly when working with various plant extracts, indicating that Ag NPs can physically interact with the cell surfaces of various bacteria. The Ag NPs action on the cell is based on numerous factors, including adherence to the bacterial cell wall and membrane, penetration into the cell and disruption of intracellular organelles and macromolecules, induction of oxidative stress, and regulation of signaling pathways. Gram-negative bacteria showed the most attachment and accumulation of Ag NPs on their cell surface. Gram-negative bacteria have a water-filled channel called porins in their outer membrane that allows Ag NPs to pass through. Porins are responsible for moving hydrophilic molecules of varied sizes and charges through the membrane in a passive manner. Because Gram-positive bacteria have a thicker cell wall that allows silver ions to penetrate the cytoplasm, the action of Ag NPs is more pronounced in Gram-negative bacteria than in Gram-positive bacteria. It's also likely that the presence of lipopolysaccharides adds to the structural integrity of Gram-negative bacteria cell walls, making them more susceptible to silver nanoparticles due to the lipopolysaccharides' negative charge, which increases Ag NP adherence. Furthermore, it is thought that when silver nanoparticles come into contact with bacteria, they produce free radicals that damage the cell membrane, causing it to become porous.

CONCLUSIONS

Ag NPs were effectively synthesized using a simple green approach. The structural, morphological, optical, elemental, topographical, and chemical features as synthesized nanomaterials were investigated using XRD, FE-SEM, TEM, EDX, and AFM and FTIR techniques. The photodegradation efficiency of RhB dye increased in general with extended period irradiation, higher photocatalyst loading up to 1.0 g/L, and decreased initial dye concentration. Furthermore, in the photocatalytic system, radical scavenging studies revealed that Ag maintained good photocatalytic activity, with hydroxyl radicals and positive holes as the predominant reactive species. Photocatalysis was found to be 78 percent effective.

Acknowledgement: The authors express their thankfulness to the Al-Mustaqbal University College for the support provided to accomplish this study>

REFERENCES

1. Wei, Z., et al., A review on phytoremediation of contaminants in air, water and soil. *Journal of hazardous materials*, 2021. 403: p. 123658.

2. Khan, S., et al., Global soil pollution by toxic elements: Current status and future perspectives on the risk assessment and remediation strategies—A review. *Journal of Hazardous Materials*, 2021. 417: p. 126039.

3. Usman, M., et al., Modeling financial development, tourism, energy consumption, and environmental quality: Is there any discrepancy between developing and developed countries? *Environmental Science and Pollution Research*, 2021. 28(41): p. 58480-58501.

4. Kapoor, D. and M.P. Singh, Heavy metal contamination in water and its possible sources, in *Heavy metals in the environment*. 2021, Elsevier. p. 179-189.

5. Saravanan, A., et al., Effective water/wastewater treatment methodologies for toxic pollutants removal: Processes and applications towards sustainable development. *Chemosphere*, 2021. 280: p. 130595.

6. Taoufik, N., et al., Comparative overview of advanced oxidation processes and biological approaches for the removal pharmaceuticals. *Journal of Environmental Management*, 2021. 288: p. 112404.

7. Saidulu, D., et al., A review on occurrences, eco-toxic effects, and remediation of emerging contaminants from wastewater: special emphasis on biological treatment based hybrid systems. *Journal of Environmental Chemical Engineering*, 2021. 9(4): p. 105282.

8. Rajoria, S., M. Vashishtha, and V.K. Sangal, Treatment of electroplating industry wastewater: a review on the various techniques. *Environmental Science and Pollution Research*, 2022: p. 1-51.

9. Isa, E.D.M., et al., Photocatalytic Degradation with Green Synthesized Metal Oxide Nanoparticles—A Mini Review. *Journal of Research in Nanoscience and Nanotechnology*, 2021. 2(1): p. 70-81.

10. Zaccaria, M., et al., Mechanistic Insight from Full Quantum Mechanical Modeling: Laccase as a Detoxifier of Aflatoxins. *bioRxiv*, 2021: p. 2020.12.31.424992.

11. Laps, S., G. Satish, and A. Brik, Harnessing the power of transition metals in solid-phase peptide synthesis and key steps in the (semi) synthesis of proteins. *Chemical Society Reviews*, 2021. 50(4): p. 2367-2387.

12. Heinemann, M.G., et al., Biogenic synthesis of gold and silver nanoparticles used in environmental applications: A review. *Trends in Environmental Analytical Chemistry*, 2021. 30: p. e00129.

13. Goga, M., et al., Biological activity of selected lichens and lichen-based Ag nanoparticles prepared by a green solid-state mechanochemical approach. *Materials Science and Engineering: C*, 2021. 119: p. 111640.

14. Garcia, R.A., et al., Cellulose, Nanocellulose, and Antimicrobial Materials for the Manufacture of Disposable Face Masks: A Review. *Bioresources*, 2021. 16(2).

15. Khodakarami, M. and M. Bagheri, Recent advances in synthesis and application of polymer nanocomposites for water and wastewater treatment. *Journal of Cleaner Production*, 2021. 296: p. 126404.

16. Ameen, F., et al., A review on metal-based nanoparticles and their toxicity to beneficial soil bacteria and fungi. *Ecotoxicology and Environmental Safety*, 2021. 213: p. 112027.

17. Patil, A.P. and K.H. Kapadnis, Antibacterial Applications of Biosynthesized AgNPs: A Short Review (2015-2020). *Material Science Research India*, 2021. 18(2): p. 143-153.

18. Mohammadzadeh, V., et al., Applications of plant-based nanoparticles in nanomedicine: A review. *Sustainable Chemistry and Pharmacy*, 2022. 25: p. 100606.

19. Xu, Y., et al., Preparation and Electrochemical Study of Ag Nanoparticles Decorated on Gallium Arsenide as Photocatalyst for Methyl Orange Degradation Under Visible Light. *Int. J. Electrochem. Sci*, 2022. 17(2024): p. 2.

20. Zhang, H., et al., Green synthesis of Ag nanoparticles from *Leucis aspera* and its application in anticancer activity against alveolar cancer. *Journal of Experimental Nanoscience*, 2022. 17(1): p. 47-60.

21. Jiali, C., et al., Synthesis of Ag-decorated vertical graphene nanosheets and their electrocatalytic efficiencies. *Plasma Science and Technology*, 2022.

22. Rezaei, F. and M. Dinari, Novel covalent organic polymer-supported Ag nanoparticles as a catalyst for nitroaromatics reduction. *Colloids and Surfaces A: Physicochemical and Engineering Aspects*, 2021. 618: p. 126441.

23. Zhu, D.-Z., et al., Laser stripping of Ag shell from Au@ Ag nanoparticles. *Rare Metals*, 2021. 40(12): p. 3454-3459.

24. Yan, J., A review of sintering-bonding technology using Ag nanoparticles for electronic packaging. *Nanomaterials*, 2021. 11(4): p. 927.

25. Bruna, T., et al., Silver nanoparticles and their antibacterial applications. *International Journal of Molecular Sciences*, 2021. 22(13): p. 7202.
26. Ojemaye, M.O., S.O. Okoh, and A.I. Okoh, Silver nanoparticles (AgNPs) facilitated by plant parts of *Crataegus ambigua* Becker AK extracts and their antibacterial, antioxidant and antimalarial activities. *Green Chemistry Letters and Reviews*, 2021. 14(1): p. 51-61.
27. Yu, P., et al., Inactivation and change of tetracycline-resistant *Escherichia coli* in secondary effluent by visible light-driven photocatalytic process using Ag/AgBr/g-C₃N₄. *Science of the Total Environment*, 2020. 705: p. 135639.